SUPPORTING INFORMATION

Time-dependent negative capacitance effects in $Al_2O_3/BaTiO_3$ bilayers

Yu Jin Kim,[1] Hiroyuki Yamada,[2] Taehwan Moon,[1] Young Jae Kwon,[1] Cheol Hyun An,[1] Han Joon Kim,[1] Keum Do Kim,[1] Young Hwan Lee,[1] Seung Dam Hyun,[1] Min Hyuk Park,[1] and Cheol Seong Hwang[1]*

[1]Department of Materials Science & Engineering and Inter-University Semiconductor Research Center, Seoul National University, Republic of Korea, [2]National Institute of Advanced Industrial Science and Technology (AIST), Higashi 1-1-1, Tsukuba, Ibaraki 305-8562, Japan.

(To be used with: *Time-dependent negative capacitance effects in $Al_2O_3/BaTiO_3$ bilayers,* Y. J. Kim et al.)

I. Negative capacitance theory

The negative capacitance behavior in dielectric/ferroelectric (DE/FE) structure had been intensively studied for the last decade. However, the theoretical understanding on the NC effects is still rather unclear, which may arise from the complexity of ferroelectricity with the nonlinear dynamics. The theoretical work reported by Khan et al. [S1] suggested the simple linearly-combined-Landau energy model assuming the homogeneous polarization in whole DE/FE structure. While this work is worth receiving credit for qualitatively expecting the emergence of NC effects in DE/FE structure, it possessed some limitation in precisely explaining the voltage amplification effects during NC operation.[S2]

Kim et al. [S2] recently reported an alternative method to explain the probable NC effect from the DE/FE structure by considering the depolarization phenomena in the FE layer. According to the report, the uncompensated spontaneous polarization charge at the DE/FE interface induces the additional electric field across the DE and FE layer, which are denoted as E_{int} and E_{dep}, respectively, and can be expressed as

$$E_{\text{int}} = -\frac{\sigma_i - P_s}{\varepsilon_0 \cdot l_d} \cdot \left(\frac{\varepsilon_b}{l_f} + \frac{\varepsilon_d}{l_d} \right)^{-1} \quad (1)$$

$$E_{dep} = \frac{\sigma_i - P_s}{\varepsilon_0 \cdot l_f} \cdot \left(\frac{\varepsilon_b}{l_f} + \frac{\varepsilon_d}{l_d} \right)^{-1} \quad (2)$$

where, and l_f (l_d) is the thickness of the FE (DE) layer; ε_b (ε_d) is the dielectric constant of the FE (DE) layer; ε_0 is permittivity of vacuum and σ_i is the compensate charge density at the DE/FE interface. (In this work, σ_i value was set to be zero. The influence of σ_i on the NC effects was intensively discussed in Ref. S2.) Using equation (2) and the Landau-Devonshire equation of FE materials, the free energy of FE layer in DE/FE system can be defined as

$$U_f = \alpha P_s^2 + \beta P_s^4 + \gamma P_s^6 - \left[E_{ext}{}^f \cdot P_s + \frac{\sigma_i \cdot P_s - \frac{1}{2} P_s^2}{\varepsilon_0 \cdot l_f} \cdot \left(\frac{\varepsilon_b}{l_f} + \frac{\varepsilon_d}{l_d} \right)^{-1} \right] \quad (3)$$

where, α, β and γ are Landau-Devonshire coefficients of a FE material, and the $E_{ext}{}^f$ is the portion of external field applied over the FE layer. It is noted that the equation (3) is valid only when the FE layer has single domains structure and homogeneous polarization. The theory was applied to an idealized model system of 25nm-$SrTiO_3$ (STO)/50nm-$BaTiO_3$ (BTO) shown below.

Figure S1a shows the U_f of the STO/BTO bilayer structure. The red lines in Figure S1 exhibit the calculation result from Khan et al.'s model. The material parameters for calculation was taken from Refs. S1 and S2. Especially, the dielectric constant of STO layer was assumed as constant (=300) over the voltage range for simplicity. As shown in Figure S1a, two models commonly reveal that the NC region (P~0) of BTO layer can be stabilized due to the presence of the interposed STO layer. Hence, the capacitance enhancement effect is expected in both models, which is calculated by using the capacitance relationship; $C=(d^2U/dP^2)^{-1}$ (Figure S1b).

However, the electric field distribution shows a clear difference between two models. According to the model by Khan et al., the electric field of each layer should be equal, hence, the voltage amplification effects cannot be involved under this formalism. In contrast, the Kim et al.'s model can account for the voltage amplification effects which can be ascribed to the depolarization field effect. As shown in Figure S2, the internal field, resulting from the charge mismatch at the DE/FE interface, can increase the electric field of DE layer to the values higher than the applied field value. At the same time, the electric field of FE layer decrease due to the presence of large depolarization field.

A further detailed discussion on this NC model can be found in Ref. S3.

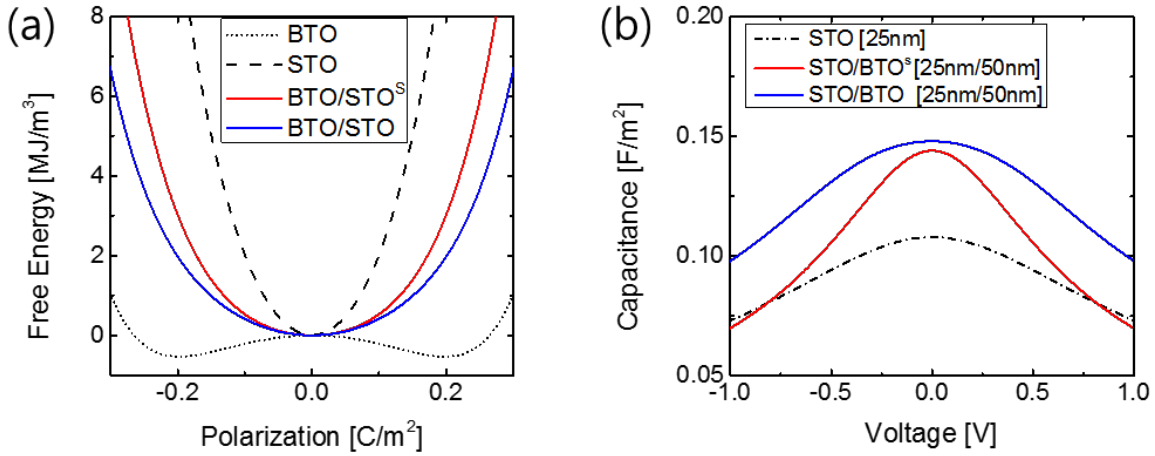

Figure S1 (a) Landau free energy diagrams and (b) capacitance-voltage characteristics of 25nm-STO /50nm-BTO bilayer system. The superscript "s" means the calculation results using method of Khan et al. [S1]

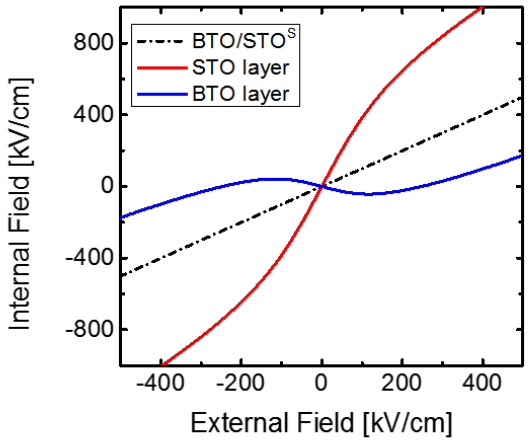

Figure S2 Electric fields of each layers in 25nm-STO /50nm-BTO bilayer system as a function of external field.

II. Q-V characteristic calculation

The spontaneous polarization – electric field (P_s-E) equation of the ferroelectric (FE) layer in the DE/FE structure with the epitaxial strain considered is written as follows [S2]:

$$\begin{aligned} E_{ext,FE} &= 2(\alpha+\eta_3)P_s + 4(\beta+\eta_{33})P_s^3 + 6\gamma P_s^5 - \frac{\sigma_i - P_s}{\varepsilon_0 \cdot l_f}\cdot\left(\frac{\varepsilon_b}{l_f}+\frac{\varepsilon_d}{l_d}\right)^{-1}, \\ &= 2(\alpha+\eta_3)P_s + 4(\beta+\eta_{33})P_s^3 + 6\gamma P_s^5 - E_{dep} \end{aligned} \tag{4}$$

where $E_{ext,FE}$ is the effective external field across the FE layer, which is assumed as constant over the FE layer; α, β and γ are the Landau coefficients of the FE material; and the ferroelastic coefficients (η_3 and η_{33}) can be expressed as $\eta_3=-(2\zeta_{12}\delta_s)/(s_{11}+s_{12})$ and $\eta_{33}=\zeta_{12}/(s_{11}+s_{12})$, where ζ_{12} and δ_s are the electrostrictive coefficient and biaxial strain, respectively, and s_{11} and s_{12} are elastic compliances. In addition, ε_0 represents the vacuum permittivity; l_d and ε_d are the thickness and relative dielectric constant of the DE layer, respectively; l_f and ε_b are the thickness and background dielectric constant of the FE layer; and σ_i is the charge density at the DE/FE interface. The last term in equation (4) corresponds to the depolarization field being induced by the uncompensated P_s in the FE layer. From this relation, the total electric field of the FE layer can be determined as the sum of the external electric field and the depolarization field ($E_{ext,FE}+E_{dep}$). It is noteworthy that the uncompensated polarization charge also induced an additional field into the DE layer. The Q-V relation can be derived using equation (4) with the continuum theory and Kirchhoff's voltage law, as in the following steps:

$$\begin{aligned} D(P_s) &= D_{DE} = D_{FE} - \sigma_i = \varepsilon_0\varepsilon_b(E_{ext,FE}+E_{dep}) - \sigma_i \\ &= P_s + \varepsilon_0\varepsilon_b(2(\alpha+\eta_3)P_s + 4(\beta+\eta_{33})P_s^3 + 6\gamma P_s^5) - \sigma_i \end{aligned} \tag{5}$$

$$\begin{aligned} V(P_s) &= l_f E_{ext,FE} + l_d E_{ext,DE} = \left(l_f + \varepsilon_b\frac{l_d}{\varepsilon_d}\right)E_{ext,FE} \\ &= \left(l_f + \varepsilon_b\frac{l_d}{\varepsilon_d}\right)\left[2(\alpha+\eta_3)P_s + 4(\beta+\eta_{33})P_s^3 + 6\gamma P_s^5 - \frac{\sigma_i - P_s}{\varepsilon_0\cdot l_f}\cdot\left(\frac{\varepsilon_b}{l_f}+\frac{\varepsilon_d}{l_d}\right)^{-1}\right] \end{aligned} \tag{6}$$

where D and V are the electric displacement and total applied voltage, respectively; and $V(P_s)$ is an odd polynomial function of P_s with all positive coefficients. Therefore, an inverse function

of $V(P_s)$ can be defined in the entire range of V (equation (6)). By combining equation (5) and the inverse function of equation (6), the D(V) can be determined for a DE/FE bilayer structure. Assuming a constant imprint voltage (V_{im}) for a given DE/FE system (i.e., $V_{im} \neq f(V)$), the Q-V relation can be defined as follows:

$$Q(V) = D(V - V_{im}) - D(V = 0) \quad (7)$$

The dashed lines in Figure 3a and the solid line in Figure 3b of main text show the simulated Q-V curves using equation (7), where α=3.3(T=-368.5)×10^5 $C^{-2}m^2N$; β=1.37×10^8 $C^{-4}m^6N$; γ=2.76×10^9 $C^{-6}m^{10}N$ [S3]; ζ_{12}=-0.034 $C^{-2}m^4$; s_{11}=-0.012×10^{-12} m^2 N^{-1}; s_{12}=6.4×10^{-12} m^2N^{-1}[S4,S5]; δ_s=-0.01; and ε_b=50 for the epitaxial BTO films [S2]. The specific l_d values of each AO/BTO capacitor were taken from l_{AO}^* with ε_d=8.9. Each simulation was performed assuming the invariant σ_i and V_{im} over the pulse voltage, with the specific σ_i values being -0.13, -0.15, and -0.17 C/m^2, and the V_{im} values being 4, 4.5, and 4.7 V for the AO thicknesses of 5, 8, and 10 nm, respectively.

III. Stability of NC operation in pulse-tests

The stability of NC operation was further confirmed by applying a series of pulses with different voltages in the 8-nm-thick AO/BTO capacitor. As shown in Figure S3a, the Q_d values from the +8 to the +12 V pulses were almost constant up to 1,000 pulses (500 ns pulse length), which indicates that stable NC operation can be achieved under such short and relatively weak pulse condition. A pulse voltage of +16 V, however, induced progressive polarization switching (charge injection), which can be confirmed by the upsurge of the non-zero Q_{res} value, as shown in Figure S3b. Hence, the Q_d value of +16 V progressively decreased with the increasing pulse number, and becomes lower than that of the +14 V pulse case when the pulse number becomes higher than ~200. Unexpectedly, the Q_d and Q_{res} values of the +14 V pulse slightly increased at the initial stage, and the +14 V Q_d value did not show a noticeable change even when the Q_{res} value became almost identical to the +16 V pulse case at pulse > ~200. This phenomenon is believed to be related with the depoling effects during the long interval (~1 sec) between the pulses. For the case of +14 V, the partly switched domains recovered their original configuration during the interval because the switched domains were not fully stabilized due to the insufficient charge injection. For the case of +16 V, however, the already-well-stabilized

switched domains remained switched during the same period, and permanent Q_d loss occurred. This can be more evidently understood from the variation of Q_c with the switching cycles shown for +12, +14, and +16 V in Figure S3b (right vertical axis). The initially very high Q_c for the +16 V case was due to the involvement of permanent polarization switching, which cannot be fully recovered during the subsequent cycles, resulting in the loss of the charging effect.

III. Hysteretic behavior in Q_d-V curves

The hysteretic behavior in the Q_d-V curves of the 8-nm-thick AO/BTO capacitor was also investigated by applying stepwise pulse trains (pulse length at each voltage: 500 ns), as shown in the Figure S3c inset picture. The directions of the Q_d-V curves are indicated by the numbered arrows in the figure. Up to the ±14 V pulse, there were negligible changes in the Q_d-V curve, and as such, no hysteresis was observed, which is consistent with the above results. At the ±16 V pulse, hysteresis started to be shown mainly within the positive-voltage region, due to partial switching, which also increased the absolute amount of Q_d in the negative-bias region. As the pulse voltage increased to ±18 V, a clearly hysteretic curve was shown, suggesting that FE switching occurred. Figure S3d shows the variation in the Q_{res}, which is consistent with the charge-injection-induced FE switching model. Based on the relation between Q_d-V and Q_{res}-V in Figures S3c and d, it was confirmed that the excessive charge injection at the sufficiently high voltage induced the hysteresis behavior and eliminated the NC effects in the AO/BTO capacitor. In addition, the initial charging state could not be recovered after applying a -18 V pulse. This phenomenon is believed to be attributable to the damage of the AO layer due to the high leakage current level or the space charge redistribution within the BTO layer. It could be also possible that very slow process within the structure including the migration of defects or domain walls was involved even after the excessive voltage pulses were removed.

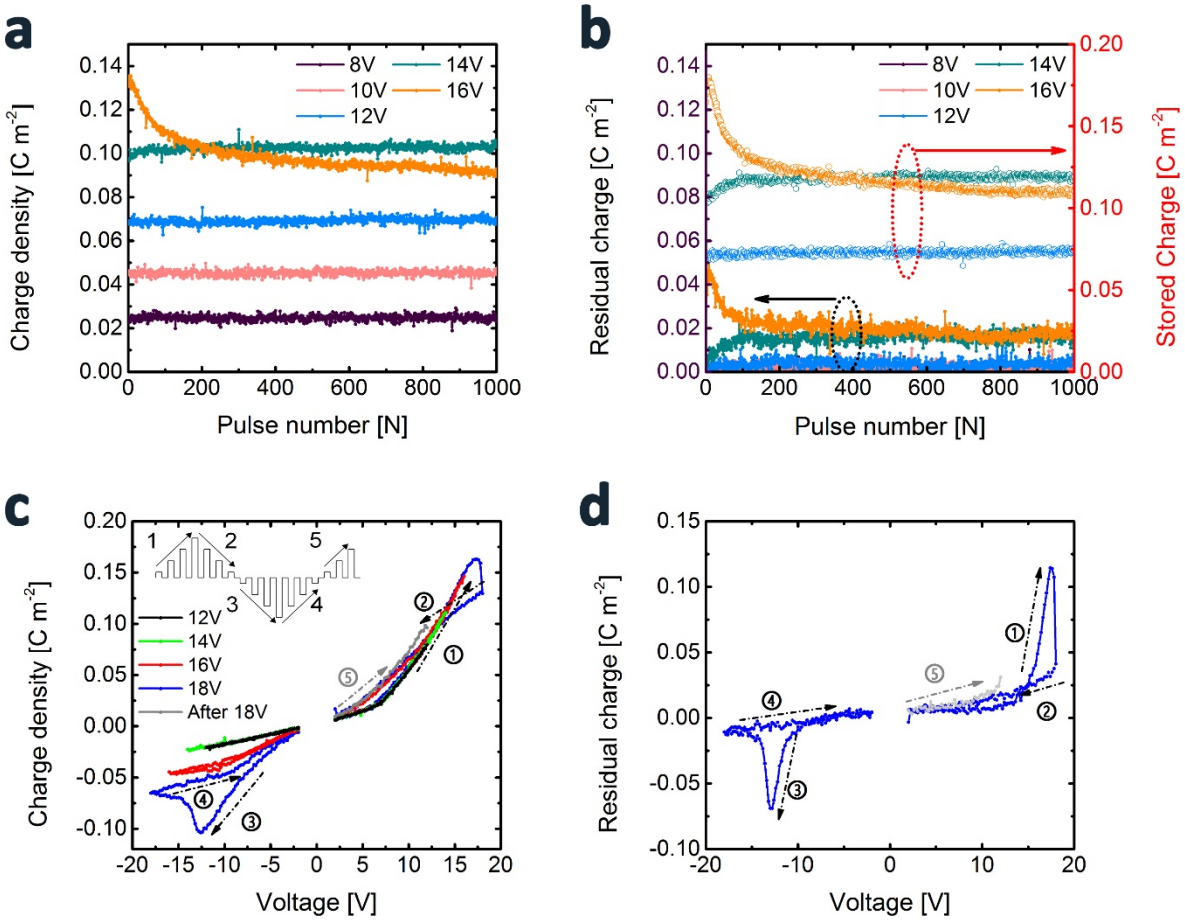

Figure S3. (a)Released charge density, (b) residual charge density (left vertical axis), and stored charge density (right vertical axis) of the 8-nm-thick AO/BTO capacitor as a function of the pulse numbers with the pulse voltage as a parameter. (c) Released charge density of the 8-nm-thick AO/BTO capacitor measured using a stepwise increasing and decreasing pulse train, as shown the inset figure with various pulse voltages. (d) Residual charge density of the 8-nm-thick AO/BTO capacitor from the stepwise pulse train with a ±18 V pulse voltage.

Reference

[S1] Khan, A. I.; Bhowmik, D.; Yu, P.; Kim, S. J.; Pan, X.; Ramesh, R.; Salahuddin, S. *Appl. Phys. Lett.* **2011**, 99, 113501.

[S2] Kim, Y. J.; Park, M. H.; Lee, Y. H.; Kim, H. J.; Jeon, W.; Moon, T.; Kim, K. D.; Jeong, D. S.; Yamada, H.; Hwang, C. S. *Sci. Rep.* **2016,** 6, 19039.

[S3] Lu, X.; Li, H.; Cao, W. *J. Appl. Phys.* **2013,** 114, 224106.

[S4] Choi, K. J.; Biegalski, M.; Li, Y. L.; Sharan, A.; Schubert, J.; Uecker, R.; Reiche, P.; Chen, Y. B.; Pan, X. Q.; Gopalan, V.; Chen, L.-Q.; Schlom, D. G.; Eom, C. B. *Science* **2004,** 306, 1005-1009.

[S5] Yamada, T. *J. Appl. Phys.* **1972,** 43, 328-338.